Uncovering quorum sensing and quenching structural properties: a systems biology approach

C. Cimolato[1], G. Selvaggio[2], M. Bellato[1], L. Marchetti[2,3], and L. Schenato[1]
[1] *Department of Information Engineering, University of Padua - Padua, Italy*
[2] *Fondazione The Microsoft Research - University of Trento COSBI - Rovereto, Italy*
[3] *Department of Cellular, Computational and Integrative Biology (CIBIO), University of Trento - Trento, Italy*

***Abstract*—Bacteria have the ability to coordinate their behavior in a cell density-dependent manner by using diffusible signal molecules. The mechanism, known as quorum sensing, is a cell-to-cell communication process exploited either by pathogens to regulate the expression of virulence and antimicrobial resistance-related genes and by synthetic biologists to engineer bacterial density-dependent functions. Using a systems biology approach, we developed a novel quorum sensing mathematical model and performed a comprehensive study of the equilibrium properties of this communication process. This analysis highlighted crucial structural properties as a result of bistability in the genetic circuit and underlined that bacteria exploit feedback control strategies to produce a unified and robust response. Due to increased antibiotic-resistant infections, researchers investigated enzymatic methods to interfere with quorum sensing. In this paper, we simulated two quorum quenching strategies. Using a modeling approach, we discovered core parameter values which guarantee the effectiveness of these strategies and could be exploited in rational design of synthetic biology based engineered bacteria.**

***Keywords*—Quorum sensing modeling, Molecular systems biology, Equilibrium analysis, Quorum quenching.**

I. INTRODUCTION

The Food and Agriculture organization of the United nations and the World health organization raked antimicrobial resistance (AMR) among the major alarming global threats to medicine and public health [1]. Up to 60% of current hospital infections are caused by AMR strains [2]. In this respect, in many pathogens, physiological processes related to AMR have proven to be strongly dependent on the population size. As a consequence, during an infection, when the population density is low, the immune system is not able to detect their presence, but, when bacterial density reaches a critical level, they exploit their communication mechanisms to coordinate their response and switch on the expression of antimicrobial resistant genes (ARGs). This unanimous response enables bacteria to overcome the immune defenses. This phenomenon is known as quorum sensing (QS). It is a cell-to-cell communication system by which bacteria can modify the expression of several ARGs based on microbial population density and consequently coordinate their response, acting together in the same manner through positive feedback regulation. Most of Gram-negative bacteria exploit similar QS networks, which are homologous to the *Vibrio Fischeri*'s LuxI/R system (hereinafter referred as Lux system). We focused on this system, not for its clinical relevance, but to leverage on the many experimental data that already exist in the literature [3].

The key element of the communication process is enclosed in the signal molecule, also called autoinducer, which is a small molecule able to quickly diffuse inside and outside the cell through the bacteria membrane. At a low cell density, communication system is in its off-state and bacteria produce the autoinducer at a basal level. As the population size grows, the autoinducer reaches a critical concentrations that moves the state of the system to the on-state, by activating the expression of ARGs and by further increasing the autoinducer synthesis.

State of the art: In light of the crucial role that QS plays in antibiotic resistance of bacteria, in the last decades, the interest of researchers focused on the development of QS mathematical models, using either a deterministic or a stochastic approach [4], and on the study of different strategies to control this cell-to-cell communication processes. The increasing threat prompted researchers to develop a new research area, focused on studying the so called quorum quenching (QQ) mechanisms, which aims to discover QS inhibitors to treat bacterial infections [5].

Contributions: In this paper, we carried out a detailed mathematical and computational analysis of the equilibrium behavior and structural properties of a deterministic mathematical model representing the proposed system, showing that bistability plays a crucial role. We then investigated two QS inhibition strategies, performing computational simulations to infer the possible system response and variations in its equilibria. To conclude, we identified key threshold parameters crucial to design and perform QQ experiments.

II. LUX QUORUM SENSING SYSTEM MODELING

A. Quorum sensing system description

Most of the QS systems are comprised of three principal elements: (i) A gene encoding for a synthase, which is an enzyme able to synthesize a specific signal molecule (autoinducer); (ii) A gene encoding for a receptor, which is a protein able to bind the same signal molecule creating an active complex; (iii) A regulated promoter inducible by the above mentioned active complex, which drives the expression of the synthase itself.

This structure implements a positive feedback loop which, up-regulating the concentration of the receptor-autoinducer complex, leads to a further increment in synthase production. Interestingly, this latter activation often involves other AMR-, pathogenic- and biofilm- related genes, thus strictly correlating

QS thresholds with the enhancement of bacterial virulence and resistance to therapies.

As an example of prototypical QS mechanism, in the Lux system (reported in Fig. 1), the gene *luxI* encodes the synthase LuxI, an enzyme which synthesizes a small signal molecule called acyl-homoserine-lactone (AHL), which can rapidly diffuse across the membrane and accumulate in and out of the cell. When it spreads inside bacteria, AHL can be detected and bounded by the dimerized form of the receptor LuxR, encoded in the gene *luxR*, constitutively expressed by the promoter (P_R); the resulting LuxR-AHL complex is able to induce the regulated promoter P_{lux}, driving the expression of *luxI* and thus closing the positive feedback loop. Previous studies suggested that the activated complex has a hetero-tetrameric structure in which two molecules of LuxR are bound to two molecules of AHL [6].

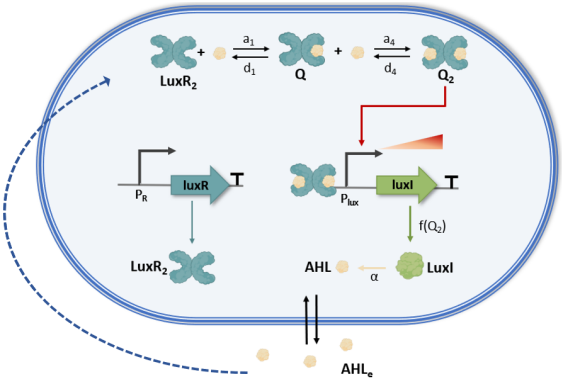

Fig. 1: Schematic of Lux quorum sensing network.

B. The model

We developed a novel cell-based dynamical model for a engineered system of Lux quorum sensing mechanism implemented in host strains of *Escherichia Coli* [6], [8] (Fig. 1):

$$\frac{dI}{dt} = \beta_{lux} + \frac{\alpha_{lux} - \beta_{lux}}{1 + \frac{K_{lux}}{Q_2}} - \gamma_I I \quad (1)$$

$$\frac{dL}{dt} = \alpha_I I - \gamma_L L + d_1 Q - K_1 d_1 R_2 L + \quad (2)$$
$$+ d_4 Q_2 - K_4 d_4 Q L + K_{15}(L_e - L)$$

$$\frac{dL_e}{dt} = K_{15}\frac{NV_I}{V - NV_I}(L - L_e) - \gamma_{L_e} L_e \quad (3)$$

$$\frac{dR_2}{dt} = d_1 Q - K_1 d_1 R_2 L \quad (4)$$

$$\frac{dQ}{dt} = K_1 d_1 R_2 L - d_1 Q - K_4 d_4 Q L + d_4 Q_2 \quad (5)$$

$$\frac{dQ_2}{dt} = K_4 d_4 Q L - d_4 Q_2 \quad (6)$$

whose parameters are summarized in Table I, where I denotes the concentration of protein LuxI, L and L_e are the intracellular and extracellular concentrations of AHL, respectively, and R_2 indicates the concentration of LuxR homodimer. Finally, Q and Q_2 define the concentrations of LuxR dimer bound to one or two molecules of AHL, respectively.

TABLE I: MODEL PARAMETERS

Symbol	*Description*	*Value*	*Units*	*Ref.*
β_{lux}	Basal LuxI synthesis rate per cell regulated by P_{lux}	0.08	$[AUmin^{-1}]$	[8]
α_{lux}	Maximum LuxI synthesis rate per cell regulated by P_{lux}	4.99	$[AUmin^{-1}]$	[8]
K_{lux}	Concentration of Q_2 corresp. to half-maximum induction of P_{lux}	194	$[nM]$	[8]
α_I	Synthesis rate of AHL	1.826	$[nMAU^{-1}min^{-1}]$	[9],[6]
R_2^{TOT}	Total concentration of dimer R_2 per cell	499.66	$[nM]$	[6]
$K_1 = \frac{a_1}{d_1}$	Equilibrium constant	0.0055	$[nM^{-1}]$	[6]
$K_4 = \frac{a_4}{d_4}$	Equilibrium constant	0.001375	$[nM^{-1}]$	[6]
K_{15}	AHL permeability rate	30	$[min^{-1}]$	[7]
γ_I	Degradation rate of LuxI	0.0173	$[min^{-1}]$	[8]
γ_L	Degradation rate of intracellular AHL	$2 \cdot 10^{-4}$	$[min^{-1}]$	[8]
γ_{L_e}	Degradation rate of extracellular AHL	$2 \cdot 10^{-4}$	$[min^{-1}]$	[8]
V_I	*E.coli* volume	1.1	$[\mu m^3]$	[12]
V	Culture environment volume	1	$[mL]$	[-]

The LuxI rate equation (Eq. 1) is composed by β_{lux}, which corresponds to the basal synthesis rate at the off-state, an inducible synthesis term which depends on the concentration of the complex Q_2, and a degradation term with spontaneous degradation rate γ_I. The Q_2-dependent synthesis rate is described as a Hill equation where α_{lux} is the maximum synthesis rate per cell and K_{lux} corresponds to the AHL concentration to reach the half-maximum synthesis rate.

In Eq. 2, α_I is the AHL synthesis rate and γ_L denotes its degradation rate. a_1 and d_1 are, respectively, the forward and reverse rate constants for the binding and unbinding reactions of the first AHL molecule to the LuxR homodimer. The equilibrium constant for this reaction is defines as $K_1 = a_1/d_1$. The forward and reverse rates describing the second AHL binding reaction are defined by a_4 and d_4, respectively. We assumed that the AHL binding and unbinding probability to the sites of R_2, Q and Q_2 are equal, therefore $a_4 = \frac{a_1}{2}$ and $d_4 = 2d_1$ implies that $K_4 = \frac{a_4}{d_4} = \frac{K_1}{4}$, where K_4 is the equilibrium constant of the second binding reaction. The last term in Eq. 2 counts the diffusion process of the autoinducer across the membrane and K_{15} is the AHL permeability rate of the *E. coli* wall [7]. Eq. 3 describes the dynamics of extracellular AHL, where N is the number of spatially homogeneous bacteria in the culture, V_I is the volume of a single *E.coli* and V is the entire culture environment volume. The degradation rate of L_e is described by γ_{L_e}.

Since LuxR is constitutively produced, we assumed R_2 has already reached its steady-state concentration. For this reason, its synthesis and degradation terms were omitted from Eq. 4. Moreover, in Eqs. 5 and 6 degradation terms for Q and Q_2 are neglected since the binding of AHL on the LuxR homodimer stabilizes the latter.

Below are the R_2 and L conservation of mass laws:

$$R_2^{TOT} = R_2 + Q + Q_2 = R_2^{TOT}(0) \quad (7)$$

$$L^{TOT} = L + Q + 2Q_2 \quad (8)$$

It is worth noticing that, since LuxR is produced at a constant basal rate, once it reaches its steady-state level, its total concentration can be assumed unchanged.

C. Deciphering the equilibrium properties of a QS system

In this section, we performed the analysis of the equilibrium behavior of the set of Eqs. 1-6. The following assumptions were made: reactions to form complexes Q and Q_2 and vice versa are reasonably much faster than the others. Under this assumption, Q and Q_2 immediately reach their steady state values and, exploiting the quasi-steady state approximation and the conservation law in Eq. 7, the model Eqs. 1-6 can be reduced to the following system:

$$\frac{dI}{dt} = \beta_{lux} + \frac{\alpha_{lux} - \beta_{lux}}{1 + \frac{K_{lux}}{Q_2}} - \gamma_I I \tag{9}$$

$$\frac{dL}{dt} = \alpha_I I - \gamma_L L + K_{15}(L_e - L) \tag{10}$$

$$\frac{dL_e}{dt} = K_{15}\frac{NV_I}{V - NV_I}(L - L_e) - \gamma_{L_e} L_e \tag{11}$$

$$Q_2 = \frac{\frac{K_1^2}{4}L^2}{1 + K_1 L + \frac{K_1^2}{4}L^2} R_2^{TOT}. \tag{12}$$

To investigate the equilibrium behavior, we assumed the steady state of all intracellular processes of the above system, by setting Eqs. 9-11 equal to 0. After some manipulations, this leads to the following equilibrium conditions:

$$L_e = \frac{\Delta}{\Delta + \gamma_{L_e}} L, \qquad L = \underbrace{\frac{\alpha_I}{\gamma_L - \Psi}}_{=:\chi} I, \tag{13}$$

where $\Delta = K_{15}\frac{NV_I}{V - NV_I}$ and $\Psi = K_{15}(\frac{\Delta}{\Delta + \gamma_{L_e}} - 1)$. Now, rewriting Q_2 as a function of LuxI:

$$Q_2 = \frac{\frac{K_1^2}{4}\chi^2 I^2}{1 + K_1 \chi I + \frac{K_1^2}{4}\chi^2 I^2} R_2^{TOT}, \tag{14}$$

where $\chi = \frac{\alpha_I(\frac{K_{15}NV_I}{V - NV_I} + \gamma_{L_e})}{(\frac{K_{15}NV_I}{V - NV_I} + \gamma_{L_e})\gamma_L + K_{15}\gamma_{L_e}}$, and substituting Eq. 14 into Eq. 9, the steady state levels of LuxI are obtained by solving the following equation:

$$\frac{dI}{dt} = \beta_{lux} + \frac{(\alpha_{lux} - \beta_{lux})(\frac{K_1}{2}\chi I)^2}{(\frac{K_1}{2}\chi I)^2 + \frac{K_{lux}}{R_2^{TOT}}(1 + \frac{K_1}{2}\chi I)^2} - \gamma_I I = 0. \tag{15}$$

It is worth noting that the equilibria of the system strongly depend on the number N of cells inside the culture environment. For this reason, we computed the solution pairs (I, N) of Eq. 15 for different values of N. Fig. 2 displays the bifurcation diagram of the steady state LuxI concentration per cell against the population density.

For low values of cell density, the system has one stable equilibrium point corresponding to a the basal concentration of LuxI (off-state). Increasing the population density, the system exhibits three different steady states, two of them stable and one unstable. The further increase in cell density brings the system back to a single stable equilibrium point, this time corresponding to a high LuxI concentration per cell (on-state).

Moreover, the bacteria colony exhibits hysteretic behavior: the system response is not simply a function of the cell density, but it also depends on its history. Indeed, the cell density level at which the communication process switches on is higher than the one at which switches off, conferring robustness to the communication process.

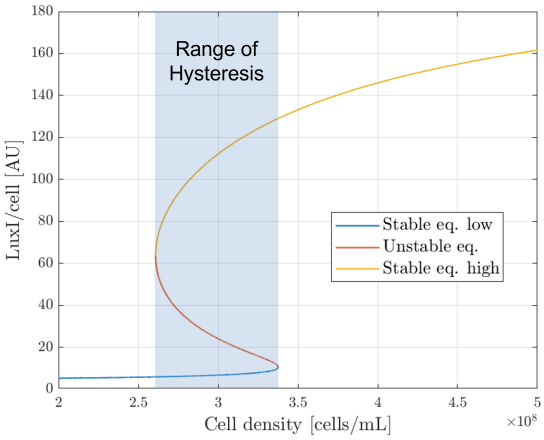

Fig. 2: Bifurcation diagram of LuxI.

III. Quorum Quenching

To address the problem of increasing antimicrobial resistant bacteria, researchers developed novel therapeutic techniques, some of which based on QQ i.e., the inhibition of bacterial communication [2]. In the QS pathway, there are several possible sites where it is possible to interfere. In this work, we explored the following two strategies to destroy AHL communication system: (i) Degradation of the extracellular AHL molecule, exploiting AHL-degrading enzymes which prevent the accumulation of extracellular AHL, as exploited in [8]; (ii) Sequestration of the AHL-receptor protein via antagonist compounds, as studied in [10].

A. QQ simulation via parameter sensitivity analysis

We exploited the developed model and the equilibrium analysis just performed to evaluate the effectiveness of these two therapeutic strategies. We addressed the problem from a parametric point of view, increasing or decreasing specific parameters which resembled the possible effect of the intended therapeutic strategy. Indeed, the degradation of the extracellular AHL can be numerically simulated by increasing the degradation rate γ_{L_e} of Eq. 3. On the other hand, the sequestration of LuxR dimer antagonizes its interaction with AHL to form complexes Q and Q_2 and it is equivalent to reduce binding rates a_1 and a_4 or, equivalently, the equilibrium constants K_1 and K_4. Results are reported in Fig. 3.

B. Critical parameter thresholds identification

Our goal is to simulate the effect of the described inhibition mechanisms and to find the key threshold values of γ_{L_e} and $K_{1,4}$ that prevent the activation of quorum sensing, even at high population sizes. In nature, there is an upper limit on the cell density that can be reached in the culture environment. Therefore, to destroy QS communication, it is sufficient to

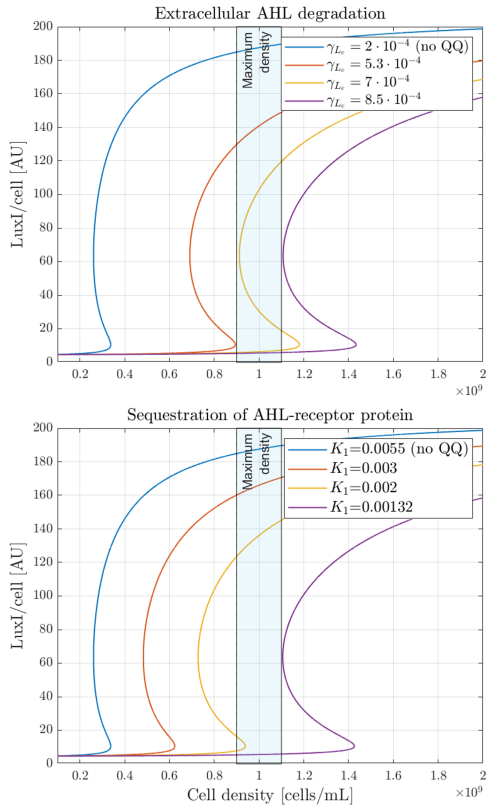

Fig. 3: QQ simulation highlighting critical parameter values forcing off-states. Top: AHL degradation. Bottom: receptor sequestration.

require that the autoinducer synthesis remains at the basal level until the maximum density is reached. In this way, the QS system cannot be activated at any feasible cell density. In literature, the maximum value of *E.coli* cell density found is around $1.1 \cdot 10^9$ cells/mL [11] and, using a conservative approach, this is the upper limit that we considered in our analysis. We simulated the two QS blocking strategies described above varying the corresponding parameters and, in Fig. 3 the resulting LuxI bifurcation diagrams are illustrated. Note that, with the parameter values corresponding to the purple curves, we reached our goal: at all feasible cell densities the system has a unique stable equilibrium which corresponds to the basal level of autoinducer. Therefore, $\gamma_{L_e} > 8.5 \cdot 10^{-4}$ min^{-1} or $K_1 < 1.32 \cdot 10^{-3}$ nM^{-1} guarantee the inhibition of QS.

These simulations clearly indicate that QS switching from off-state to on-state strictly depends on the population size: while each bacterium must produce a sufficiently low amount of AHL to avoid self-activation of QS, on the other they must produce enough autoinducer to switch on QS once the threshold cell density has been reached. This behavior strongly depends on the hysteretic curve displayed in Fig. 2 and is a consequence of the underlying positive feedback loop.

The effort required to activate the communication process is considerable, and hysteresis ensures that once triggered, it is more difficult to reverse it by a cell density decrease. Indeed, our analysis proved that the system requires a significantly lower level of cell density to reset the autoinducer production to the basal level, compared to the QS activating threshold one. This finding confirms that bacteria exploit control strategies to perform disturbance rejection to cell density variations. In this case, the positive feedback ensured robustness to autoinducers perturbations and reduced susceptibility to noise.

IV. Conclusion

Due to the rise in antibiotic resistance and the need to prevent new emergence of such strains, there will be in the near future a progressive application of synthetic biology studies exploiting QQ enzymes and CRISPR interference [13], [14]. This will enable the development of new therapeutic approaches against AMR bacteria and a better understanding of the structural properties of QS mechanisms. In this regard, this work identified key threshold parameters that are essential for designing and carrying out quorum quenching experiments, highlighting design requirement for pharmacological- and synthetic biology-based therapeutic approaches.

Acknowledgement

This work was funded by Fondazione Cariparo grant "Bando Ricerca Scientifica di Eccellenza 2021 n59576" and by University of Padova, Department of Information Engineering, PhD Grant PON-RI 2014-20 (CCI2014IT16M2OP005) on FSE REACT-EU funds. The authors thank B. Di Camillo and S. Del Favero for the helpful discussions.

References

[1] FAO, Drivers, dynamics and epidemiology of antimicrobial resistance in animal production, 2016. Link
[2] P. Williams, Quorum sensing: an emerging target for antibacterial chemotherapy?, *Expert Opin Ther Targets*, 6(3):257–274, 2002. Link
[3] M. E. Taga, B. L. Bassler, Chemical communication among bacteria, *Proc Natl Acad Sci*, 100:14549-14554, 2003. Link
[4] J. Pérez-Velazquez, M. Golgeli, Mathematical modelling of bacterial quorum sensing: A review, *Bull Math Biol*, 78:1585–1639, 2016.Link
[5] S. Zhong, S. He, Quorum sensing inhibition or quenching in Acinetobacter baumannii: the novel therapeutic strategies for new drug development, *Front Microbiol*, 12:558003, 2021. Link
[6] L. Pasotti, M. Bellato, D. De Marchi, P. Magni, Mechanistic models of inducible synthetic circuits for joint description of DNA copy number, regulatory protein level, and cell load", *Processes*, 7(3):119, 2019. Link
[7] X. Li, J. Jin, X. Zhang, F. Xu, J. Zhong, et al., Quantifying the optimal strategy of population control of quorum sensing network in Escherichia coli, *npj Systems biology and applications*, 7(1):1-16, 2021. Link
[8] L. Pasotti, et al., A synthetic close-loop controller circuit for the regulation of an extracellular molecule by engineered bacteria, *IEEE Trans Biomed Circuits Syst*, 13(1):248-258, 2019. Link
[9] A. L. Schaefer, D. L. Val, B. L. Hanzelka, J. E. Cronan, E. P. Greenberg, Generation of cell-to-cell signals in quorum sensing: acyl homoserine lactone synthase activity of a purified Vibro fischeri LuxI protein, *Proc Natl Acad Sci*, 93(18):9505-9509, 1996. Link
[10] G. Bernabè, et al., A novel phenolic derivative inhibits AHL-dependent quorum sensing signaling in Pseudomonas aeruginosa, *Front Pharmacol*, 13:996871, 2022. Link
[11] P. Mira, P. Yeh, B. G. Hall, Estimating microbial population data from optical density, *Plos one*, 17(10):e0276040, 2022. Link
[12] H. E. Kubitschek, J. A. Friske, Determination of bacterial cell volume with the Coulter Counter, *J Bacteriol*, 168(3):1466-1467, 1986. Link
[13] H. H. Huang, et al., dCas9 regulator to neutralize competition in CRISPRi circuits, *Nat Commun*, 12(1):1-7, 2021. Link
[14] M. Bellato, et al., CRISPR Interference Modules as Low-Burden Logic Inverters in Synthetic Circuits, *Front Bioeng Biotechnol*, 9:1513, 2022. Link